Characterization of the optically stimulated luminescence (OSL) response of beta-irradiated alexandrite-polymer composites.

M. C. S. Nunes[1], L. S. Lima[2], E. M. Yoshimura[2], L. V. S. França[3], O. Baffa[3], L. G. Jacobsohn[4], A. L. M. C. Malthez[5], R. Kunzel[6], N. M. Trindade*[1,2]

[1] Department of Physics, Federal Institute of Education, Science and Technology of São Paulo, São Paulo, SP, Brazil.

[2] Institute of Physics, University of São Paulo, São Paulo, SP, Brazil.

[3] Department of Physics, FFCLRP, University of São Paulo, Ribeirão Preto, SP, Brazil.

[4] Department of Materials Science and Engineering, Clemson University, Clemson, SC, USA.

[5] Department of Physics, Federal University of Technology – Paraná, Curitiba, PR, Brazil.

[6] Department of Physics, Federal University of São Paulo, Diadema, SP, Brazil.

*email: ntrindade@ifsp.edu.br

ABSTRACT

Alexandrite mineral ($BeAl_2O_4:Cr^{3+}$) powder, incorporated in a fluorinated polymer, was prepared in the form of pellets. A mixture with 20 wt% of the alexandrite in the pellet had the luminescence behavior evaluated as a function of exposure to ionizing radiation using the optically stimulated luminescence (OSL) technique. The OSL measurements were evaluated in terms of dose-response (beta dose from 0.1 to 5 Gy), repeatability, reproducibility, and fading. The results showed that the OSL intensity signal varied linearly with the irradiation dose and that the OSL intensity suffered a strong reduction during the first five days of storage in the dark but remained stable for at least the following 30 days. Radioluminescence (RL) measurements under X-ray excitation revealed a weak luminescence within the ultraviolet-visible spectral region, while optical absorption (OA) measurements revealed the presence of Cr^{3+} impurities.

Keywords: alexandrite; polymer; dosimetry; OSL; radioluminescence.

1. INTRODUCTION

Dosimetric materials are useful for evaluating personal and environmental doses as well as irradiation doses received in medical, spatial and safety activities [1,2]. Particularly, natural dosimeters like minerals find application, *e.g.*, in retrospective dosimetry, geological and archeological dating [3]. Also, natural materials can be a low-cost alternative to the synthetic ones, and may be more readily available in large quantities [2,4]. Brazil has the world´s largest deposit of alexandrite ($BeAl_2O_4:Cr^{3+}$) [5]. In addition, chrysoberyl ($BeAl_2O_4$) host contains ~ 20 wt.% BeO and ~ 80 wt.% Al_2O_3:C [6], both commercially available as luminescent dosimeters. Within this context, the potential of natural alexandrite as a dosimetric material has been investigated by luminescence techniques such as optically stimulated luminescence (OSL) [7]. This fact, together with Z_{eff} = 10.8 value, which is lower than that of Al_2O_3:C, a widely used dosimeter, makes alexandrite an interesting candidate for investigation as a natural OSL dosimetric material. The development of a functional and low-cost radiation detector is one of the goals of this investigation.

OSL has been established as a reliable dosimetry technique for many years [8]. OSL corresponds to the luminescence emitted by some materials previously exposed to ionized radiation stimulated by the absorption of optical energy [1]. OSL emission arises from the recombination at the luminescence centers of charges optically released from specific traps. Therefore, OSL intensity can be related to the absorbed radiation dose [1,9,10]. There are three major modes of stimulation of the material in OSL readout, consisting of: continuous-wave OSL (CW-OSL) [1,9], linear modulation OSL (LM-OSL) [11] and time-resolved luminescence [12,13]. CW-OSL, used in this work, is a very popular technique as it requires simpler instrumentation and yields a good signal-to-noise ratio [14]. The OSL signal obtained under stimulation with constant light power (CW-OSL) is observed as a progressive decrease in time (decay curve) as

charges are released from the traps [9,15]. The simplest first-order model for OSL processes assumes the absence of re-trapping such that all charges escaping from the traps immediately recombine producing luminescence. Consequently, OSL intensity is proportional to the variation in the concentration of trapped charges, and in the case of CW-OSL it is described by the following equation (1):

$$I_{cw}(t) = \sum_i n_{0,i}\alpha_i e^{(-\alpha_i t)} \quad (1)$$

where $I_{cw}(t)$ is the OSL intensity at time t, n_{0i} is the initial trapped charge concentration at type *i* trap , and α_i is the escape probability of trap *i*, defined as the product of the photon flux φ (photons per unit time per unit area) and the photoionization cross section σ_i, *i.e.*, $\alpha_i = \sigma_i\varphi$. This product describes the probability of a photon with energy *hv* to release a trapped charge interacting with a particular defect [9]. From the values of the escape probability (α_i), the respective time constant τ_i of OSL decay curve may also be defined by equation (2):

$$\tau_i = \frac{1}{\alpha_i} \quad (2)$$

OSL dosimetry presents several advantages such as high efficiency and stable sensitivity, accuracy, possibility of reevaluation of irradiation doses, fast read-out and no thermal annealing steps, as compared to other techniques used in personal and environmental dosimetry [1,16,17]. Currently, BeO and Al_2O_3:C are the OSL materials mostly used for personal dosimetry [1,18,19]. However, the discovery and development of new OSL dosimetric materials is necessary [20–23].

Likewise, radioluminescence (RL) is an important tool for studying luminescence mechanisms. RL corresponds to the luminescence emitted by a material under exposure to ionizing radiation [24,25]. The differences in the luminescence mechanisms between RL and OSL allows

RL to provide insight into the nature of the luminescence centers and thus to complement OSL in the development of new luminescent dosimeters [1,26].

This work focused on the characterization of a composite based on powdered alexandrite mineral dispersed in a fluorinated polymer serving as a binder. Among the characteristics of the composite, the reproducibility and repeatability of the OSL response were evaluated. The dosimetric response to beta irradiation up to 5 Gy and the deconvolutions of the OSL curves, as well as RL and optical absorption of this composite are being reported here for the first time.

2. MATERIALS AND METHODS

Alexandrite-polymer composites were fabricated as follows: firstly, an alexandrite mineral sample, extracted from a Brazilian mine, was manually crushed and powdered using a porcelain mortar and pestle (Chiarotti Ltda), followed by sieving (Granutest Ltda) obtaining micrometric grains (< 0.35 mm). The sieved alexandrite powder was thermally treated at 400 °C for 1 h to erase any signal previously accumulated due to natural irradiation and left to cool naturally to room temperature. Then the powder was mixed with an organic matrix based on a fluorinated polymer. The OSL signal of irradiated fluorinated polymer serving as the binder was previously evaluated, and no OSL signal is detected for doses up to 5 Gy. In this work, 5 pellets with 20 wt% alexandrite were investigated. Fig. 1 shows the pellets, which presented a smooth surface and light brown color.

Figure 1: Alexandrite – polymer pellets arranged on stainless steel sample holders.

For optical absorption (OA) and RL measurements, besides the composite pellets described above, both a natural and a synthetic alexandrite samples were used, along with a pellet of the fluorinated polymer. The synthetic alexandrite single crystal was grown by the Czochralski method [27] with Cr^{3+} doping for up to 0.3 at.% substituting for $A1^{3+}$ [28]. The single crystal had parallel faces and thickness of 2.33 mm. The natural alexandrite sample was taken from the powder after sieving (grain size <75μm).

OSL measurements were carried out at room temperature using an automated Risø TL/OSL reader, model DA-20, DTU Nutech. The OSL signal was stimulated in CW mode using blue LEDs (470 nm, FWHM = 20 nm, 80 mW/cm^2). The OSL signal was detected by a bialkali photomultiplier tube through a 7.5 mm thick Hoya U-340 filter (transmission band 250 - 390 nm, FWHM), and a mask with 5 mm diameter. For each OSL measurement, three samples were readout for 60s twice for completely erasing any signal. Irradiation was executed using the built-in $^{90}Sr/^{90}Y$ beta (10 mGy/s) source of the TL/OSL reader delivering a cumulative dose within 0.1 to 5 Gy. The OSL decay curves were analyzed with OriginLab software by fitting experimental

data with Eq. 1 using a of Levenberg Marquardt algorithm [29,30]. The background signal of the measurements was considered as an additive constant.

For the repeatability evaluation, one sample was irradiated to 1 Gy followed by readout and this procedure was repeated 10 times for the same sample. In the reproducibility evaluation, 5 samples were all irradiated to 1 Gy followed by readout at the same conditions. The coefficient of variation, $CV(\%) = \frac{SD}{mean} \times 100$, where SD is the standard deviation, was used to evaluate the repeatability and reproducibility tests of the OSL response. Fading tests were performed for 3 different storage times (1hour, 5 days and 30 days) after irradiation to 1 Gy in the dark using the same pellet. After irradiation, the individual samples were covered with light-tight black plastic to prevent any possible light incidence. Packing of the sample with black plastic was performed under low-intensity red light.

OA measurements were performed in reflectance mode in the range from 350 to 750 nm using a Shimadzu 2600 series UV-Vis spectrophotometer, except for the synthetic sample when it was performed with a Varian Cary 17 in transmittance mode, taking advantage of the sample's transparency. The OA data were recorded using non-irradiated samples.

RL measurements were executed at room temperature using a home-made apparatus composed of a 0.2 mA Moxtek, Inc. Magnum 50 kV X-ray source with tungsten target, and an Ocean Optics USB2000 spectrometer coupled to an optical fiber [24]. The light emitted by the sample (350 to 850 nm) was collected by a collimating lens focused into the optical fiber (74-series Collimating Lenses, Ocean Optics). Each RL spectrum was collected during 30s under continuous wave (CW) X-ray irradiation (dose rate = 92 mGy/s). The spectra presented in this work correspond to the total intensity accumulated over the whole collection time.

3. RESULTS AND DISCUSSION

An important parameter for a dosimetric applications is the lower limit of detection. Usually, the minimum detectable dose (D_0) is calculated by equation (3):

$$D_0 = (\overline{B} + 3\sigma_{\overline{B}}) \cdot f_c \qquad (3)$$

where $\overline{B}$ is the mean OSL background signal from the samples, $\sigma_{\overline{B}}$ is the standard deviation of measurement of the mean background and f_c is the calibration factor that is obtained from the inverse of the slope of the OSL response [31,32]. For the composites fabricated in this work, a D_0 of ~ 75 mGy was obtained.

Fig. 2 shows the average OSL decay curves obtained from the measurement of samples, varying the irradiation dose from 0.1 to 5 Gy. Each decay curve corresponds to the average of the decay curves of three pellets irradiated to the same dose.

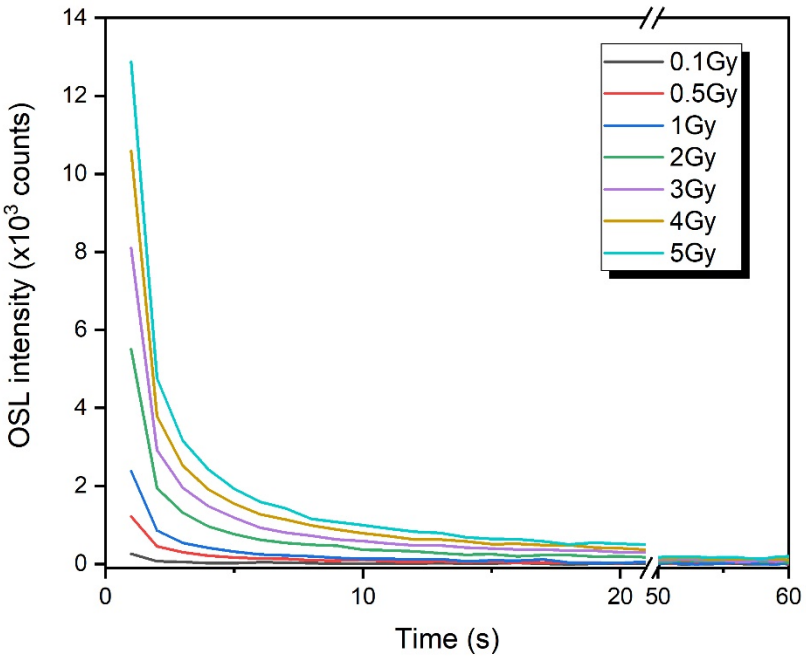

Figure 2: OSL decay curves after different doses of beta irradiation.

All decay curves showed the same shape, regardless the irradiation dose. In all cases, about 20s of illumination were enough to essentially extinguish the signal. The average of the OSL signal of the three samples as a function of the irradiation dose is shown in Fig. 3. Also shown is the linear best fit. The best fitting procedure yielded a linear coefficient of $(-6.7 \pm 5.9) \times 10^1$ counts and a slope of $(2.64 \pm 0.03) \times 10^3$ counts Gy^{-1}, with $R^2 = 0.99$, where R^2 is the coefficient of determination. Note that the coefficient of determination is very close to 1, that is, there is a strong correlation (*i.e.*, small variance) between the OSL signal and the irradiation dose. In dosimetry, a linear dose-response relationship is a highly desired outcome since it is decisive criterium to whether or not investigate a material as a dosimeter.

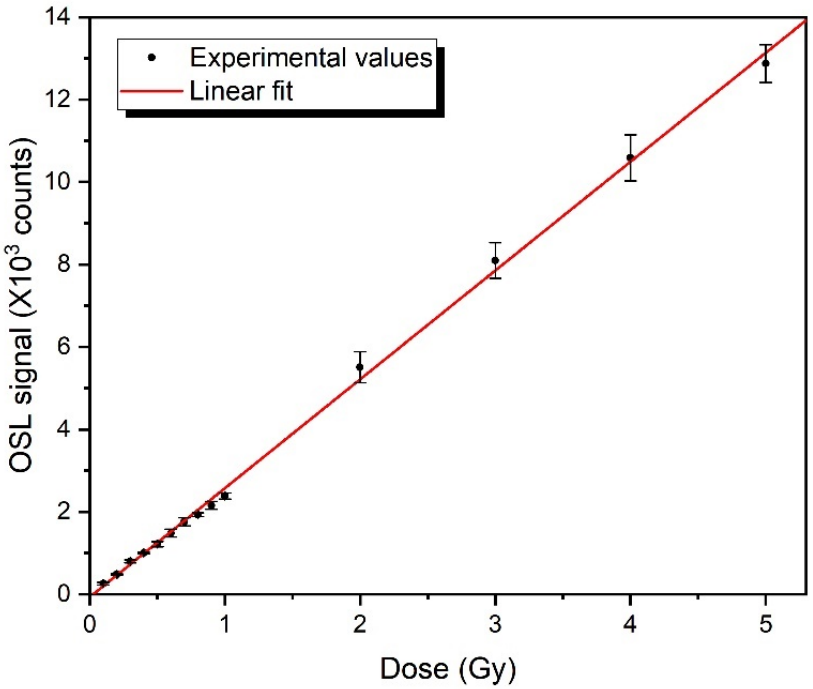

Figure 3: OSL signal as a function of the beta irradiation dose. Each point is the mean value of three different pellets, the error bars correspond to the standard deviation of the three values, and the straight line corresponds to the linear fitting.

The OSL decay curves were fitted with decaying exponential functions (*cf.* Eq. 1). However, it was not possible to obtain reliable fittings for doses smaller than 1 Gy due to the relatively low signal-to-noise ratio of those results. Fig. 4 illustrates an example of the fitting for the OSL decay curve obtained after 3Gy of beta irradiation dose. The exponential curves can be characterized as fast (blue curve), medium (black curve) and slow (green curve) decay components. Note that the sum of the components (red curve) is very close to the experimental results. Importantly, for all the irradiation doses between 1 and 5 Gy, three exponential decay components were necessary to obtain fittings with a correlation coefficient $R^2 > 0.985$.

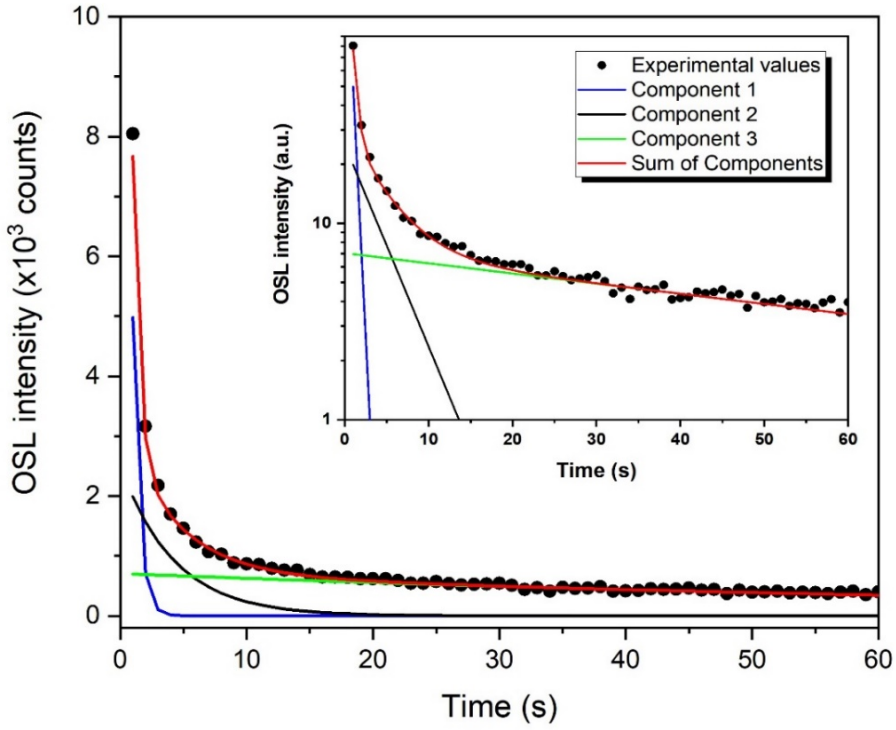

Figure 4: Example of deconvolution of the CW-OSL curve of a composite irradiated with 3Gy, with 3 exponential decay components: component 1 (blue line), component 2 (black line) and component 3 (green line). The dots represent the experimental results and the red line is the sum of all components. The inset is a semi-logarithmic scale representation for better visualization.

The values of n_0 for each of the components are plotted against the beta irradiation dose in Fig. 5. As the trends look linear, reliable linear fittings with $R^2 > 0.998$ for fast component; $R^2 > 0.993$ for medium component and $R^2 > 0.974$ for slow component, were obtained. It is important to mention that τ values were constant for the same component and all irradiation doses. In the dose range investigated, the CW-OSL curves present yielded three time constants: the fast with τ_1=0.51 s, the medium with τ_2=4.2 s, and the slow with τ_3=84 s.

The behavior of n_0 as a function of irradiation dose seen in Fig. 5 corroborates the linear dose response observed in Fig. 3. In addition, the trapped charge concentration (n_0) in the defects related to the slow component is higher than in the other two components, being about 2/3 of the total trapped charges. This result is probably connected to the dosimetric traps corresponding to the main thermoluminescent peaks of alexandrite centered on 225 and 270 ºC, as reported in the literature [33,34].

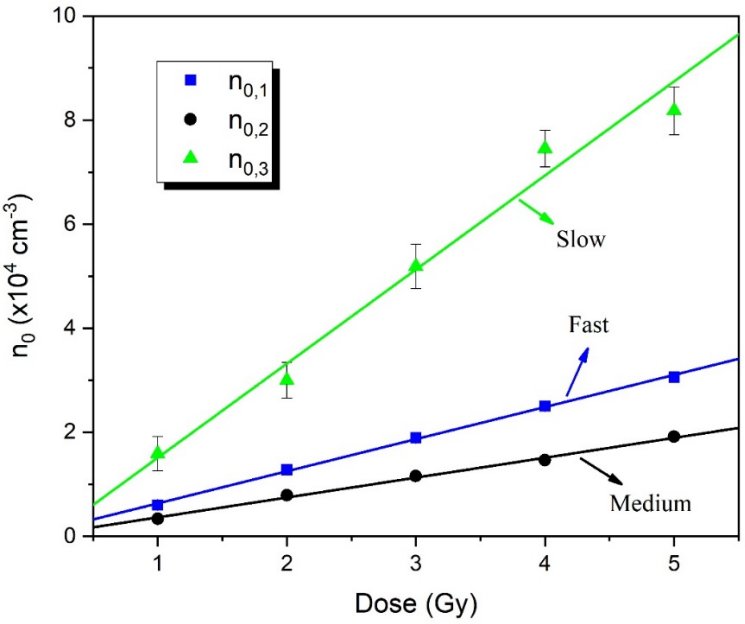

Figure 5: Parameter n_0 as a function of beta radiation dose. The τ values represented in the graph is constant for each component for all irradiation doses.

Using the intensity values normalized by the corresponding value obtained immediately after 1Gy irradiation, the reduction of the OSL signal (fading) of the sample was investigated for storage periods of 1 hour, 5 days and 30 days. The OSL signal fades up to 40% of the initial intensity value in the first hour of the storage period, at room temperature, and under dark conditions. In the next 5 days, the signal decreases by another 20%. The results after 30 days of storage show no additional fading, with the signal being stable at 40% of the original value.

In order to test the repeatability of the OSL signal, a sequence measurement was carried out using a same pellet. The OSL signal was found to be repeatable when re-measured under the same conditions, as the *CV* value of 2.3% was obtained, without trends in the observed results. In terms of reproducibility of the OSL signal in the 5 pellet-batch, a *CV* of 8.2% was obtained. The optically opaque nature of the binder (cf. Fig. 1) suggests that the origin of the OSL signal is restricted to the surface of the pellets and thus it is strongly affected by the concentration of mineral particles on the surface of the pellet, that is stochastic. With this result we conclude that the use of these composite dosimeters is possible, but a pre-evaluation of each pellet would be required for a better precision of dose determination, and further work will focus on obtaining more homogeneous batches of composite pellets.

Recently, our group investigated the chemical composition of the natural samples from the same batch used in this study by scanning electron microscopy and energy-dispersive X-ray spectroscopy measurements [35]. This analysis leads us to conclude that the alexandrite phase is predominant in the mineral with the presence of Cr (0.90 wt.%) and Fe (1.25 wt.%) impurities in the sample. As widely discussed before in the literature [33,34,36–40], Cr^{3+} - Cr^{3+} pairs and clusters, and Fe^{3+} are responsible for the optical and luminescent properties of alexandrite. Within this context, the optical absorption spectrum for the samples was measured, at room temperature.

It is shown in Fig. 6.

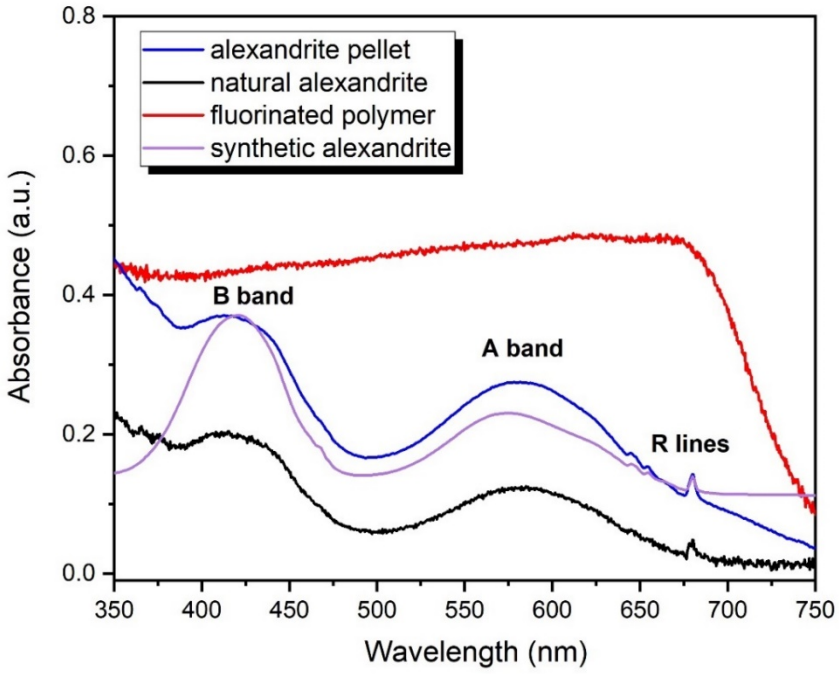

Figure 6: Optical absorption spectra of the synthetic and natural alexandrite samples as well as of a pellet of alexandrite powder composite, and a fluorinated polymer pellet.

In alexandrite samples, the visible spectra range present two overlapping lines (R lines ~ 680 nm) and two wide absorption bands, denominated A (~ 590 nm) and B (~ 420 nm). A Band represents Cr^{3+} ions and B band represents Cr^{3+} and Fe^{3+} incorporated in two distinct aluminum sites; Al_1 and Al_2 [39,41,42]. In addition, R lines appear precisely at the same wavelengths, in both absorption and emission spectra reported previously [43–45]. Fig. 6 also shows that the powder presents the same optical absorption bands as the synthetic alexandrite sample, therefore, the quality of the natural samples has been certified. Also, the production of the composite pellets has no influence on the sample optical absorption spectrum in the visible range, since the synthetic sample, powder and pellets present the bands at the same positions of the spectrum. The results

also suggest that the increasing absorption observed below ~400 nm is mostly due to the alexandrite mineral.

RL measurements were executed to gain insight into the existing OSL recombination centers. The spectrum of the 20% alexandrite - composite (blue line) is shown in Fig. 7 together with the spectra of the fluorinated polymer binder (red line), as well as natural (black line) and synthetic (purple line) alexandrite. The fluorinated polymer binder did not present any RL signal. The comparison of the spectra of the natural sample with the synthetic one that is doped with, Cr^{3+} suggests that the 680 nm band is due to Cr^{3+}. However, it is possible to observe that the band centered at 680 nm is broader in the natural sample than in the synthetic sample, indicating that it might be attributed not to only to Cr^{3+} but also to Fe^{3+}. The other band centered at about 570 nm, that occurs only for the natural samples, is probably related to an additional impurity. Previous chemical analysis of this mineral revealed the presence of several impurities, and particularly of Mn [33], and the emission of Mn^{4+} from alexandrite revealed a broad band around 560 nm, among other bands [36]. Importantly, a weak contribution below ~400 nm can be seen from the composite. The low intensity was attributed in part to the opaque nature of the binder as well as to very low efficiency of the optical detector is in this spectral region. This emission is attributed to many defects in the alexandrite mineral known to luminesce in this region [6].

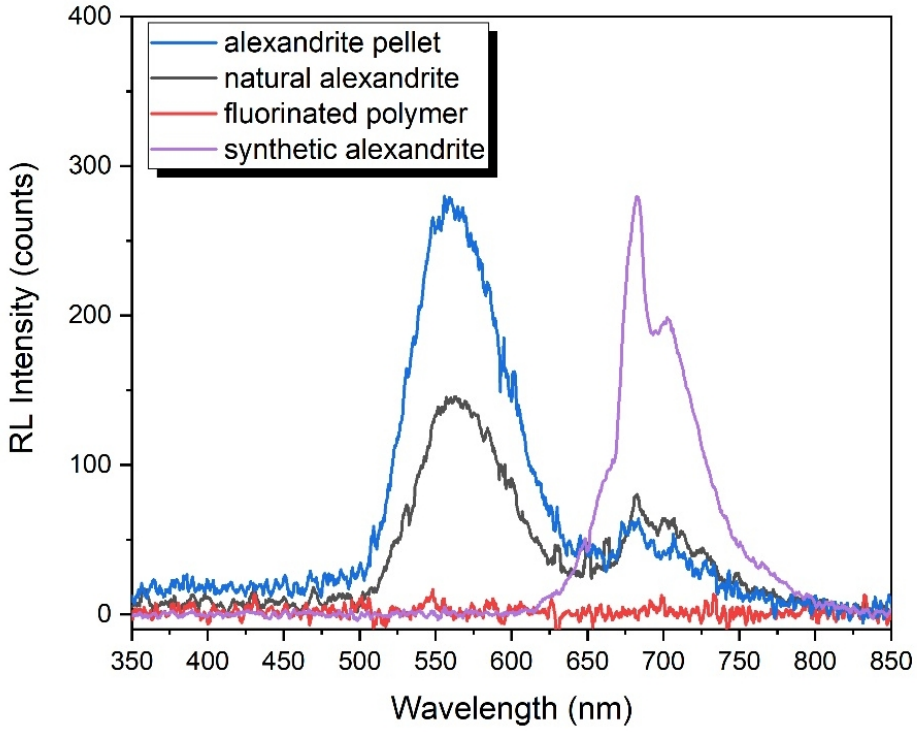

Figure 7: RL spectra of the synthetic and natural alexandrite as well as alexandrite composite and fluorinated polymer pellets.

4. CONCLUSIONS

In this work we investigated a new composite material for OSL dosimetric applications, based on powder of alexandrite mineral (20 wt.%) dispersed in a fluorinated polymer binder. OSL intensity signal from the produced pellet varies linearly with the irradiation dose between 0.1 and 5 Gy and keeps 40% of the original signal stable after 30 days of storage in the dark. The repeatability results show a good *CV* (2.3% for one sample), and the reproducibility presents a *CV* about 8%. The analysis of the components of the OSL decay curves showed that for doses ranging from 1 to 5Gy, the curve is composed by 3 exponential decay components, fast (0.5s), medium (4.2s) and slow (84s). These fittings were able to describe very well the experimental curves, showing a determination coefficient very close to 1 for all cases. Optical absorption and RL

showed that Cr, Fe and Mn ions are mainly responsible for luminescence in the visible spectrum. In addition, RL measurements revealed the presence recombination centers in the UV that are expected to be responsible for the detected OSL signal. Future work will focus on improving the fabrication procedure to achieve better reproducibility among different pellets and higher UV emission.

ACKNOWLEDGMENTS

M. C. S. Nunes is grateful to São Paulo Research Foundation (FAPESP), grant #2018/16894-4. E. M. Yoshimura is grateful to São Paulo Research Foundation (FAPESP), grant #2018/05982-0 and National Council for Scientific and Technological Development (CNPq), grant #306843/2018-8. O. Baffa thanks National Council for Scientific and Technological Development (CNPq), grant #407471/2016-2. L. G. Jacobsohn is grateful to National Science Foundation, grant #1653016. N. M. Trindade is grateful to São Paulo Research Foundation (FAPESP), grant #2019/05915-3.

REFERENCES

[1] E.G. Yukihara, S.W.S. Mckeever, Optically Stimulated Luminescence: Fundamentals and Applications, UK: John Wiley and Sons, West Sussex, 2011.

[2] S.S. Lalic, D.N. Souza, O. Baffa, F. D´Errico, New dosimetric materials for applications in medical physics, Rev. Bras. Física Médica. 13 (2019) 10. https://doi.org/10.29384/rbfm.2019.v13.n1.p24-33.

[3] J.M. Kalita, G. Wary, Thermoluminescence properties of minerals and their application, LAP LAMBERT Academic Publishing, Saarbrucken, Germany, 2016.

[4] D.N. Souza, M.E.G. Valerio, J.F. de Lima, L.V.E. Caldas, Dosimetric properties of natural brazilian topaz: A thermally stimulated exoeletronic emission and thermoluminescence study, Nucl. Instruments Methods Phys. Res. Sect. B Beam Interact. with Mater. Atoms. 166–167 (2000) 209–214. https://doi.org/10.1016/S0168-583X(99)00746-6.

[5] M.S. Basilio, A. Pedrosa-Soares, H. Jordt-Evangelista, Depositos de alexandrita de Malacacheta, Minas Gerais., Rev. Geonomos. 8 (2000) 8. https://doi.org/10.18285/geonomos.v8i1.147.

[6] V.Y. Ivanov, V.A. Pustovarov, E.S. Shlygin, A. V Korotaev, A. V Kruzhalov, Electronic

excitations in $BeAl_2O_4$, Be_2SiO_4, and $Be_3Al_2Si_6O_{18}$ crystals, Phys. Solid State. 47 (2005) 466–473. https://doi.org/10.1134/1.1884706.

[7] N.M. Trindade, A.L.M.C. Malthez, A. de Castro Nascimento, R.S. da Silva, L.G. Jacobsohn, E.M. Yoshimura, Fabrication and characterization of a composite dosimeter based on natural alexandrite, Opt. Mater. (Amst). 85 (2018) 281–286. https://doi.org/10.1016/j.optmat.2018.08.066.

[8] S.W.S. McKeever, Optically stimulated luminescence dosimetry, Nucl. Instruments Methods Phys. Res. Sect. B Beam Interact. with Mater. Atoms. 184 (2001) 29–54. https://doi.org/https://doi.org/10.1016/S0168-583X(01)00588-2.

[9] L. Botter-Jensen, S.W.S. McKeever, A.G. Wintle, Optically Stimulated Luminescence Dosimetry, Elsevier Science, Amsterdam, 2003. https://doi.org/10.1016/B978-0-444-50684-9.X5077-6.

[10] A.S. Pradhan, J.I. Lee, J.L. Kim, Recent developments of optically stimulated luminescence materials and techniques for radiation dosimetry and clinical applications, J. Med. Phys. 33 (2008) 85–99. https://doi.org/10.4103/0971-6203.42748.

[11] E. Bulur, An alternative technique for optically stimulated luminescence (OSL) experiment, Radiat. Meas. 26 (1996) 701–709. https://doi.org/10.1016/S1350-4487(97)82884-3.

[12] M.L. Chithambo, An introduction to time-resolved optically stimulated luminescence, Morgan & Claypool Publishers, San Rafael, CA, USA, 2018.

[13] B.G. Markey, L.E. Colyott, S.W.S. Mckeever, Time-resolved optically stimulated luminescence from α-Al_2O_3:C, Radiat. Meas. 24 (1995) 457–463. https://doi.org/10.1016/1350-4487(94)00119-L.

[14] N.S. Rawat, B. Dhabekar, M.S. Kulkarni, K.P. Muthe, D.R. Mishra, A. Soni, S.K. Gupta, D.A.R. Babu, Optimization of CW-OSL parameters for improved dose detection threshold in Al_2O_3:C, Radiat. Meas. 71 (2014) 212–216. https://doi.org/10.1016/j.radmeas.2014.02.013.

[15] L. Bøtter-Jensen, Development of Optically Stimulated Luminescence Techniques using Natural Minerals and Ceramics, and their Application to Retrospective Dosimetry, University of Copenhagen, 2000.

[16] R. Chen, V. Pagonis, Thermally and Optically Stimulated Luminescence: A simulation Approach, John Wiley & Sons, West Sussex, 2011.

[17] A.L.M.C. Malthez, M.B. Freitas, E.M. Yoshimura, V.L.S.N. Button, Application of optically stimulated luminescence technique to evaluate simultaneously accumulated and single doses with the same dosimeter, Radiat. Phys. Chem. 95 (2014) 134–136. https://doi.org/10.1016/j.radphyschem.2013.02.026.

[18] E.G. Yukihara, S.W.S. McKeever, Optically stimulated luminescence (OSL) dosimetry in medicine, Phys. Med. Biol. 53 (2008) R351. https://doi.org/10.1088/0031-9155/53/20/R01.

[19] T. Yanagida, G. Okada, N. Kawaguchi, Ionizing-radiation-induced storage-luminescence for dosimetric applications, J. Lumin. 207 (2019) 14–21. https://doi.org/10.1016/j.jlumin.2018.11.004.

[20] M.W. Blair, L.G. Jacobsohn, S.C. Tornga, O. Ugurlu, B.L. Bennett, E.G. Yukihara, R.E. Muenchausen, Nanophosphor aluminum oxide: Luminescence response of a potential dosimetric material, J. Lumin. 130 (2010) 825–831. https://doi.org/https://doi.org/10.1016/j.jlumin.2009.12.008.

[21] J.R. Hazelton, E.G. Yukihara, L.G. Jacobsohn, M.W. Blair, R. Muenchausen, Feasibility of using oxyorthosilicates as optically stimulated luminescence detectors, Radiat. Meas. 45 (2010) 681–683. https://doi.org/https://doi.org/10.1016/j.radmeas.2009.09.005.

[22] E.M. Yoshimura, E.G. Yukihara, Optically stimulated luminescence: Searching for new dosimetric materials, Nucl. Instruments Methods Phys. Res. Sect. B Beam Interact. with Mater. Atoms. 250 (2006) 337–341. https://doi.org/https://doi.org/10.1016/j.nimb.2006.04.134.

[23] E.G. Yukihara, E.D. Milliken, L.C. Oliveira, V.R. Orante-Barrón, L.G. Jacobsohn, M.W. Blair, Systematic development of new thermoluminescence and optically stimulated luminescence materials, J. Lumin. 133 (2013) 203–210. https://doi.org/https://doi.org/10.1016/j.jlumin.2011.12.018.

[24] L.V.S. França, L.C. Oliveira, O. Baffa, Development of a thermoluminescence and radioluminescence integrated spectrometer, Measurement. 134 (2019) 492–499. https://doi.org/https://doi.org/10.1016/j.measurement.2018.10.101.

[25] V. Pagonis, M.L. Chithambo, R. Chen, A. Chruścińska, M. Fasoli, S.H. Li, M. Martini, K. Ramseyer, Thermal dependence of luminescence lifetimes and radioluminescence in quartz, J. Lumin. 145 (2014) 38–48. https://doi.org/https://doi.org/10.1016/j.jlumin.2013.07.022.

[26] C.M. Sunta, Unraveling Thermoluminescence, Springer India, 2015. https://doi.org/10.1007/978-81-322-1940-8.

[27] G. Xingan, C. Meiling, L. Nairen, Q. Qinghai, H. Mingfang, F. Jingwei, W. Shulin, L. Zongquan, Q. Yong, Czochralski growth of alexandrite crystals and investigation of their defects, J. Cryst. Growth. 83 (1987) 311–318. https://doi.org/http://dx.doi.org/10.1016/0022-0248(87)90292-2.

[28] J. Walling, O. Peterson, H. Jenssen, R. Morris, E.O. Dell, Tunable alexandrite lasers, IEEE J. Quantum Electron. 16 (1980) 1302–1315. https://doi.org/10.1109/jqe.1980.1070430.

[29] K. Levenberg, A method for the solution of certain non-linear problems in least squares, Q. Appl. Math. 2 (1944) 164–168. https://doi.org/10.1090/qam/10666.

[30] Origin Data Analysis and Graphing Software. Curve Fitting, n.d.

[31] M. Oberhofer, A. Scharmann, Applied thermoluminescence dosimetry, Bristol : Hilger, 1981. http://lib.ugent.be/catalog/rug01:000705616.

[32] A.M.B. Silva, D.O. Junot, L.V.E. Caldas, D.N. Souza, Structural, optical and dosimetric characterization of $CaSO_4$:Tb, $CaSO_4$:Tb, Ag and $CaSO_4$:Tb,Ag(NP), J. Lumin. (2020) 117286. https://doi.org/10.1016/j.jlumin.2020.117286.

[33] N.M. Trindade, H. Kahn, E.M. Yoshimura, Thermoluminescence of natural $BeAl_2O_4$: Cr^{3+} Brazilian mineral: Preliminary studies, J. Lumin. 195 (2018) 356–361. https://doi.org/10.1016/j.jlumin.2017.11.057.

[34] N.M. Trindade, M.R. da Cruz, H. Kahn, L.G. Jacobsohn, E.M. Yoshimura, Thermoluminescence and radioluminescence of alexandrite mineral, J. Lumin. 206 (2019) 455–461. https://doi.org/10.1016/j.jlumin.2018.10.114.

[35] S.L. Dardengo, M.C.S. Nunes, C. Ulsen, E.M. Yoshimura, N.M. Trindade, Investigação da termoluminescência de alexandrita ($BeAl_2O_4$: Cr^{3+}), Brazilian J. Radiat. Sci. in press (n.d.).

[36] M. Gafta, R. Reisfeld, G. Panckzer, Modern Luminescence Spectroscopy of Minerals and Materials, Springer Berlin, Heidelberg, New York, 2005.

[37] G.M. Ferraz, S. Watanabe, S.O. Souza, R.M.F. Scalvi, TL, EPR and Optical Absorption Studies on Natural Alexandrite Compared to Natural Chrysoberyl, Radiat. Prot. Dosimetry. 100 (2002) 471–474. https://doi.org/10.1093/oxfordjournals.rpd.a005917.

[38] K.L. Schepler, Fluorescence of inversion site Cr^{3+} ions in alexandrite, J. Appl. Phys. 56 (1984) 1314–1318. https://doi.org/10.1063/1.334119.

[39] N.M. Trindade, R.M.F. Scalvi, L.V. de A. Scalvi, Cr^{+3} Distribution in Al_1 and Al_2 Sites of Alexandrite ($BeAl_2O_4$: Cr^{3+}) Induced by Annealing, Investigated by Optical Spectroscopy, Energy Power Eng. 2 (2010) 18–24. https://doi.org/10.4236/epe.2010.21004.

[40] S.-U. Weber, M. Grodzicki, W. Lottermoser, G.J. Redhammer, G. Tippelt, J. Ponahlo, G. Amthauer, 57Fe Mössbauer spectroscopy, X-ray single-crystal diffractometry, and electronic structure calculations on natural alexandrite, Phys. Chem. Miner. 34 (2007) 507–515. https://doi.org/10.1007/s00269-007-0166-6.

[41] A.B. Suchocki, G.D. Gilliland, R.C. Powell, J.M. Bowen, J.C. Walling, Spectroscopic properties of alexandrite crystals II, J. Lumin. 37 (1987) 29–37. https://doi.org/10.1016/0022-2313(87)90179-7.

[42] R.C. Powell, L. Xi, X. Gang, G.J. Quarles, J.C. Walling, Spectroscopic properties of alexandrite crystals, Phys. Rev. B. 32 (1985) 2788–2797. https://link.aps.org/doi/10.1103/PhysRevB.32.2788.

[43] P. Fabeni, G.P. Pazzi, L. Salvini, Impurity centers for tunable lasers in the ultraviolet and visible regions, J. Phys. Chem. Solids. 52 (1991) 299–317. https://doi.org/https://doi.org/10.1016/0022-3697(91)90069-C.

[44] N.M. Trindade, A.S. Tabata, R.M.F. Scalvi, L.V. de A. Scalvi, Temperature Dependent Luminescence Spectra of Synthetic and Natural Alexandrite, Mater. Sci. Appl. 2 (2011) 284–287. https://doi.org/10.4236/msa.2011.24037.

[45] N.M. Trindade, A.R. Blak, E.M. Yoshimura, L.V. de A. Scalvi, R.M.F. Scalvi, Photo-

Induced Thermally Stimulated Depolarization Current (TSDC) in Natural and Synthetic Alexandrite ($BeAl_2O_4$: Cr^{3+}), Mater. Sci. Appl. 7 (2016) 881–894. https://doi.org/10.4236/msa.2016.712067.

Declaration of interests

 The authors declare that they have no known competing financial interests or personal relationships that could have appeared to influence the work reported in this paper.

☐The authors declare the following financial interests/personal relationships which may be considered as potential competing interests:

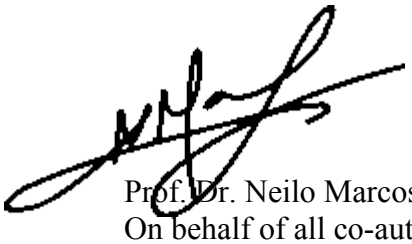

Prof. Dr. Neilo Marcos Trindade
On behalf of all co-authors

M. C. S. Nunes: Investigation, Formal analysis, Data Curation, Writing - Original Draft

L. S. Lima: Investigation, Data Curation, Writing - Original Draft

E. M. Yoshimura: Resources, Supervision, Writing-Review&Editing

L. V. S. França: Investigation, Data Curation

O. Baffa: Investigation, Supervision, Writing-Review&Editing

L. G. Jacobsohn: Supervision, Writing-Review&Editing

A. L. M. C. Malthez: Investigation, Methodology

R. Kunzel: Investigation, Data Curation

N. M. Trindade: Conceptualization, Methology, Validation, Writing - Original Draft, Writing-Review&Editing